



UNIVERSITY OF LEEDS

This is a repository copy of *The Effects of Corrosion on Particle Emissions from a Grey Cast Iron Brake Disc*.

White Rose Research Online URL for this paper:

<https://eprints.whiterose.ac.uk/193394/>

Version: Accepted Version

Proceedings Paper:

Ghouri, I, Barker, R, Brooks, P et al. (2 more authors) (2022) The Effects of Corrosion on Particle Emissions from a Grey Cast Iron Brake Disc. In: SAE Technical Papers. Brake Colloquium & Exhibition - 40th Annual, 25-28 Sep 2022, Grand Rapids, MI, USA. SAE International .

<https://doi.org/10.4271/2022-01-1178>

© 2022 SAE International. All rights reserved. No part of this publication may be reproduced, stored in a retrieval system, or transmitted, in any form or by any means, electronic, mechanical, photocopying, recording, or otherwise, without the prior written permission of SAE International. This is an author produced version of a conference paper, published in SAE Technical Papers. Uploaded in accordance with the publisher's self-archiving policy.

Reuse

Items deposited in White Rose Research Online are protected by copyright, with all rights reserved unless indicated otherwise. They may be downloaded and/or printed for private study, or other acts as permitted by national copyright laws. The publisher or other rights holders may allow further reproduction and re-use of the full text version. This is indicated by the licence information on the White Rose Research Online record for the item.

Takedown

If you consider content in White Rose Research Online to be in breach of UK law, please notify us by emailing eprints@whiterose.ac.uk including the URL of the record and the reason for the withdrawal request.



eprints@whiterose.ac.uk
<https://eprints.whiterose.ac.uk/>

The Effects of Corrosion on Particle Emissions from a Grey Cast Iron Brake Disc

Ishmaeel Ghouri*, Richard Barker*, Peter Brooks*, Shahriar Kosarieh* and David Barton*

**School of Mechanical Engineering, University of Leeds*

Reducing exhaust emissions has been a major focus of research for a number of years since internal combustion engines (ICE) contribute to a large number of harmful particles entering the environment. As a way of reducing emissions and helping to tackle climate change, many countries are announcing that they will ban the sale of new ICE vehicles soon. Electrical vehicles (EVs) represent a popular alternative vehicle propulsion system. However, although they produce zero exhaust emissions, there is still concern regarding non-exhaust emission, such as brake dust, which can potentially cause harm to human health and the environment. Despite EVs primarily using regenerative braking, they still require friction brakes as a backup as and when required. Moreover, most EVs continue to use the traditional grey cast iron (GCI) brake rotor, which is heavy and prone to corrosion, potentially exacerbating brake wear emissions. This study concentrates on emissions from a conventional grey cast iron friction brake before and after exposure to a corrosive environment. It was found that the effect of corrosion increases both the number and mass of particle emissions by over 50% and inhibits braking performance by reducing the coefficient of friction. The surface of the brake disc was also found to be affected by corrosion as many crevices and pits were formed.

1 Introduction

Over the years, there have been significant developments in reducing greenhouse gases and other air pollutants emitted from internal combustion engines (ICE) vehicles, despite an increase in total vehicle numbers each year. More firm restrictions on ICE vehicles have led to some countries placing bans on new ICE vehicle sales to help to tackle climate change [1]. With Norway being one of the first countries to plan to implement this, two-thirds of all new vehicles sold in Norway in 2021 were electric [2]. As more countries, such as the UK, Denmark, Germany, Iceland and others follow in the footsteps of Norway, banning sales of new IC vehicles will inevitably lead to a substantial increase in the number of EVs on the road [3, 4]. Despite EVs not producing any exhaust emissions, they still emit particulate matter (PM) into the environment, mainly from the wearing of brakes, tyres, road surfaces and the resuspension of road dust. PM from brakes, tyres and road surfaces is classed as non-exhaust emission. Unlike exhaust emissions, there is currently no legislation on limiting brake emissions [5, 6]. With EVs becoming more popular and the decline of ICE vehicles, it is predicted that the non-exhaust PM emission will surpass that from the exhaust [6]. One of the biggest contributors to non-exhausted emissions is the friction brake system in a vehicle. As part of the brak-

ing mechanism to slow or stop a vehicle, wear particles are released from the brakes and emitted into the environment. Brake particles not only cause pollution to the environment but pose direct risks to human health [7]. There is evidence that friction brake emissions will continue to increase with the rising number of vehicles on the road each year [8]. EVs fitted with regenerative braking show promise in being able to reduce greenhouse gases and harmful PM emitted into the environment. Instead of using pairs of friction materials to slow the vehicle down, the drive motor acts as a generator to convert the vehicle's kinetic energy into electrical energy [9]. The electrical energy generated from braking is fed back into the vehicle battery increasing the EVs range by 8 to 25% compared to vehicles without regenerative braking [10]. However, at low speeds and when the battery is nearly fully charged, the regenerative braking system becomes less efficient and the vehicle relies more heavily on the friction brakes to bring it to a final stop [11]. Thus, EVs still use friction brakes when more brake torque is needed in the event of an emergency stop or to hold the vehicle on a slope. However, with modern EVs, a sophisticated design allows the driver to utilise the regenerative braking system more frequently than the conventional friction brakes to allow for more energy to recuperate back into the battery [12, 13]. Over time the regenerative braking will be more effective and efficient, and the usage of

friction brakes will be further reduced. However, the lack of friction brake use may allow corrosion to build up on the friction material surface, potentially increasing emissions when the friction brakes are next applied. The disc brake system is an open system design to allow for airflow to cool the disc in particular. However, this poses a problem as it could allow the atmospheric environment to cause potential harm or damage to the brake system. In locations that experience a large amount of rainfall or freezing conditions, this can lead to corrosion. For example, the acidity of rainwater can have an impact on the rate of corrosion. The use of salts such as sodium chloride, magnesium chloride and calcium chloride in freezing conditions can influence the rate of corrosion [14]. When such salts are absorbed in water, concentrated chloride solutions are formed which are highly corrosive and are known to cause corrosion pits in metals even when they have protective coatings [15–17]. The most commonly used brake rotor material in road vehicles is GCI [18, 19]. GCI is used as it has good thermal and mechanical properties, however, it is also known to be prone to corrosion [20–22]. Corrosion of a GCI rotor poses potential problems as it can lead to surface degradation of the material and a potential increase in brake wear emissions. In this study, the effect of corrosion on a GCI brake disc is investigated in terms of brake temperature, coefficient of friction (COF), brake pad wear, emission particle number and mass distribution using an in-house full-scale non-inertial brake dynamometer

2 Background literature

The main function of an automotive brake system is to bring the vehicle to a stop or to slow it down in a safe and controlled manner. Friction brakes are used not only for slowing the vehicle down but also as parking brake. The friction brake system decelerates a vehicle by converting the kinetic energy into thermal energy. A rough and hard brake pad surface can lead to high levels of friction. However, there is a strong correlation between high levels of friction and increased wear rate [23]. Corrosion can affect the material properties such as causing the material to lose its strength, especially in the case of ferrous metals such as iron and steel alloys which can lead to catastrophic failures. However, in some materials, corrosion can be desirable; for example, an oxide surface layer can have increased strength and improved corrosion resistance compared with the substrate material. Examples of this include aluminium, copper, chromium and nickel alloys where an adherent oxide surface layer is formed to protect the substrate material from corrosion [24]. Montasell et al. [25] investigated vehicle judder due to corrosion of a cast iron brake rotor. It was observed that most of the corroded layer on the brake rotor was removed after the first snub test. However, even after the completion of the 3rd snub test, there were still traces of corrosion on the rotor. Cho et al. [26] also investigated the correlation between corrosion and brake judder. This study showed that a brake disc with a thicker oxide layer showed higher brake torque variation (BTV) compared with the brake disc with a thinner ox-

ide layer. Therefore, they concluded that an oxide layer formed on the brake disc surface has a strong influence on the BTV. Hamid et al. [27] investigated the frictional characteristics of a corroded grey cast iron brake disc. This study used two different brake pad materials with different material compositions against two GCI brake discs. The brake underwent a burnishing procedure to transfer some of the friction material onto the surface of the brake discs, after which both brake discs underwent a corrosion process. The results showed that the concentration and thickness of the oxide layer formed on the two burnished brake discs were different. Thus, the composition of the friction material is a factor in the formation of corrosion on the surface of the brake rotor. Montasell et al. [25] also concluded that the thickness of the corroded layer on the brake disc is affected by the material composition of the transfer layer that has been developed on the brake disc surface. There are two main sizes of particulate matter of concern when considering brake wear emissions, PM10 and PM2.5. PM10 or coarse particle matter is when the particle diameter ranges between 2.5 and 10 micrometres (µm). PM2.5 or fine particle matter is particle matter with a diameter of 2.5 micrometres (µm) or less. It is estimated that around 55% of the total non-exhaust particle matter in the PM10 size category in the urban environment comes from brake emissions and the remainder from tire and road surface debris [8]. Studies have been carried out on the health effect of brake wear emission, including the link between brake wear particles and Alzheimer's disease [28]. Magnetite, a form of iron oxide, has been found in the brains of people who had died of Alzheimer's disease and is also found in brake wear emissions. Gasser et al. [29] investigated the toxic effects of brake wear particles on epithelial lung cells in vitro. This experiment involved capturing brake wear particles from two types of braking behaviours (full stop and urban deceleration) and exposing them to lung cells. The results suggest that the brake wear particles damage tight junction cells and increased pro-inflammatory responses. Asmawi et al. [30] investigated the particle emission from a conventional GCI rotor and a lightweight aluminium alloy with an alumina coating produced by the Plasma Electrolytic Oxidation (PEO) process. It was found that the GCI brake disc produced significantly more particle mass emissions compared to the PEO-coated disc. Gramstat et al. [31] investigated particle emission from a low-steel and a copper-free Non-Asbestos Organic (NAO) brake pad material rubbing on a GCI rotor. It was found that brake emissions are not only dependent on the coefficient of friction but also on other factors such as temperature, brake pressure and the friction material used. The copper-free NAO pad material produced greater numbers of particles during high-demanding braking tests compared to the low-steel pad material. Mancini et al. [32] investigated how different brake cycles can affect the chemical composition of brake wear particle emissions. It was found that a more demanding brake cycle produced more brake emissions, such as iron oxides, than the less demanding brake cycle. Hesse et al. [33] studied the particle emission of different disc brake materials, focussing on particle emissions during the

bedding-in procedure and temperature observations. At the start of the bedding-in procedure, particle emissions were particularly high but then started to decrease. This is likely due to the protective coating being removed from the brake disc. Also, surface topography was not yet uniform and the tribolayer had not been fully formed during the initial bedding process. Hesse et al. [33] also found that, if a critical threshold temperature was exceeded during braking, this can lead to the formation of more nanoparticles. Overall, the tungsten carbide-coated GCI disc and the carbon-ceramic disc produced lower emissions compared to the standard cast iron disc

3 Methodology

3.1 Brake dynamometer set-up

The Leeds brake dynamometer consists of an air-tight enclosure that houses the brake system, see figure 1. The brake pad and disc material used for this investigation are commercial OEM components. The brake disc is a 284 mm diameter vented GCI disc and the brake pads use a semi-metallic friction material made for the Lancia Delta. The brake pads are housed in a bespoke 4 piston brake caliper, previously designed to suppress brake squeal [34]. Two K-type thermocouples are used to measure disc surface temperature at different points on the free rubbing surface. High-Efficiency Particulate Absorbing (HEPA) H14 filters are used to supply clean air into the enclosure which reduces the risk of contamination. A 4 kW fan is used to control the airflow speed. The ducting pipes are made from galvanised steel sheets which have an internal diameter of 225 mm. The airflow velocity can range from 6 to 15 m/s. A Dekati ELPI+ impactor is used to collect and measure the brake wear emission through an isokinetic probe inserted in the outlet ducting. The air sampling volume rate and the probe geometry have been tailored to provide isokinetic sampling conditions [30]. The Dekati ELPI+ is capable of measuring in real-time the particle number and mass distribution using a 14-stage impactor with particle size stages ranging from 10 μm down to 6 nm [35].

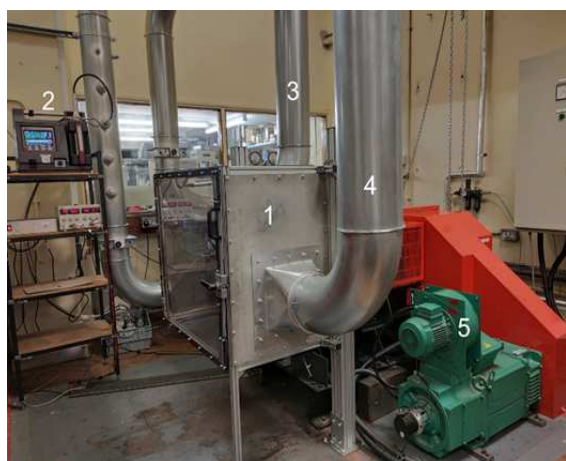


Fig. 1. Brake dynamometer set-up: 1) Enclosure. 2) Dekati ELPI+. 3) Inlet pipe. 4) Outlet pipe. 5) 45 kW motor

3.2 Salt spray cabinet set-up

The CW salt spray cabinet type SF100, shown in Figure 2, contains one atomised tower which the salt solution is sprayed from. A custom-made holder is used to mount the brake disc in the cabinet. The holder allows for the brake disc to be placed at an angle of $\pm 15^\circ$ from the vertical axis to allow for the salt solution to run-off so there is no stagnant solution on the brake disc surface.



Fig. 2. Salt spray cabinet housing a brake disc

4 Test protocol

For purpose of this investigation, only the brake disc is corroded. The test protocol for the corrosion of the brake disc follows the ASTM B117-11 standard [36] which specifies a controlled corrosive environment for a range of coated and uncoated materials. The ASTM B117 standard was preferred, to more complex standards that use cyclic climate conditions, due to its relative simplicity for this preliminary study. The salt solution is prepared by dissolving 5 parts by mass of pure sodium chloride in 95 parts of water. The pH of the atomized salt solution is within the 6.5 to 7.2 range. The salt spray cabinet is used to maintain steady-state conditions at a temperature of $35 \pm 2^\circ\text{C}$ with a relative humidity of 95%. The brake disc is placed into the salt spray cabinet as shown in Figure 2, where it is exposed to a corrosive environment for 96 hours. The brake disc is reversed within the cabinet after 48 hours, to allow for a uniform corrosion deposition. The hub of the brake disc is taped off, thus protecting it from the environment as it would be if attached to the wheel of the vehicle [25]. After the brake disc has undergone 96 hours in the salt spray cabinet, it is taken out and left to air dry in normal laboratory atmospheric conditions. For these comparative brake tests before and after corrosion, the chosen brake duty cycle is drag braking. Drag braking simulates the vehicle maintaining a constant speed on a long downhill gradient during which near steady-state temperature conditions are achieved [37]. This type of brake application was selected partly because the Leeds non-inertial dynamometer is not yet capable of simulating variable speed stops such as in the WLTP test cycle. However, it is also advantageous

when conducting comparative tribological studies to maintain constant contact pressure and sliding speed in order to achieve near steady-state friction and temperature conditions during the measurement of wear emissions. Although it could be argued that this type of test is not representative of real city driving conditions, even EVs fitted with regenerative braking may occasionally undergo a steep mountain descent under friction braking only, when for example the battery is fully charged. For this reason, the pressures applied and the disc temperatures achieved in the present comparative tests were higher than those typically experienced by EVs during normal city driving. The current brake tests consist of three drag brake applications at 5, 7.5 and 10 bar hydraulic line pressure at a constant dynamometer speed of 150 rpm. The duration of each drag braking application is 90 minutes. No braking pressure is applied for the first 600 seconds of each test to allow for the air-flow to become stable and to generate data for background particle measurement. Each 90-minute drag braking event is followed by a 5-minute cooldown period where no braking is applied in order to measure brake wear particles that may still be emitted from the brake. The complete test protocol is broken down into seven stages as shown in Figure 3. New brake pads and a new disc are first bedded in. The low brake pressure test is then repeated 3 times followed by 3 repeats of the medium and then the high-pressure tests to check for consistency in results. The brake disc is then subjected to the salt spray treatment for 96 hours. The corroded brake disc subsequently undergoes the same sequence of brake tests as it did before it was corroded. At the end of the 3 repeat tests at each pressure condition for both the corroded and uncorroded disc tests, the pads are removed from the calliper and dimensional wear measured using a micrometre with a resolution of 0.01 mm in line with the SAE J2986 standard procedure [38].

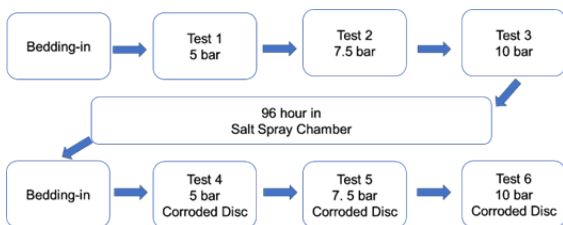


Fig. 3. Test protocol

5 Results

5.1 Brake test

Figure 4 and Figure 5 present disc surface temperature against time from the start of the test for the uncorroded and corroded rotor tests respectively. Near steady-state conditions were met for all brake pressures in both the uncorroded and corroded disc conditions at around 2000 seconds. The results show that as the brake pressure increases so does the steady-state brake temperature, as would be expected.

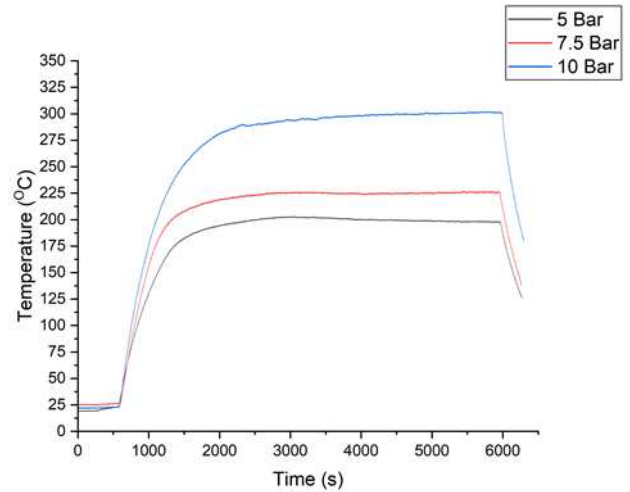


Fig. 4. Disc surface temperature for 5, 7.5 and 10 bar brake pressure for the uncorroded tests

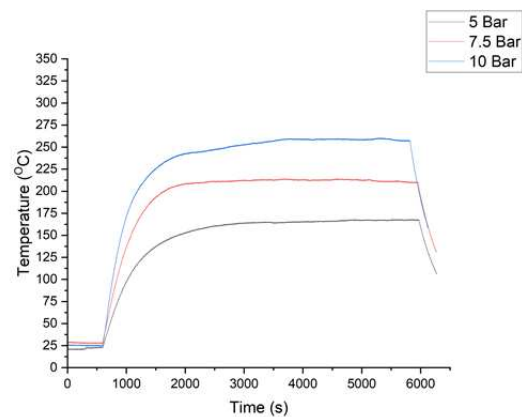


Fig. 5. Disc surface temperature for 5, 7.5 and 10 bar brake pressure for the corroded tests

Figure 6 and Figure 7 present coefficient of friction (COF) results at 5, 7.5 and 10 bar before and after the brake disc was corroded, respectively. The COF is calculated from the applied pressure and measured torque output in the usual way [39]. When the brake pressure is initially applied, there is a spike in COF, which lasts for about 1500 seconds before the COF starts to level off and becomes near steady-state. This initial spike in COF is probably due to the progressive development of the tribolayer between the pads and the disc [40, 41]. As the brake pressure increased, the steady-state COF decreases in both uncorroded and corroded tests, with 5 bar producing the highest COF and 10 bar the lowest COF in both rotor conditions. This reduction in COF is likely to be caused by a breakdown of the tribolayer as the brake pressure is increased [42].

5.2 Surface Analysis

Figure 8 presents images of the surface of the brake disc after the completion of the 3 tests at each pressure for the uncorroded disc. Figure 8a shows the new brake disc which is covered by a protective coating applied by the manufac-

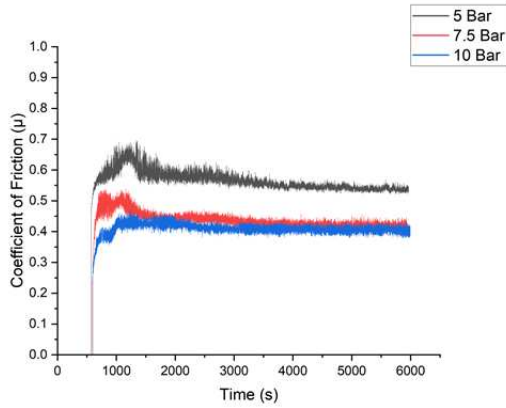


Fig. 6. COF for 5, 7.5 and 10 bar brake pressure for the uncorroded test

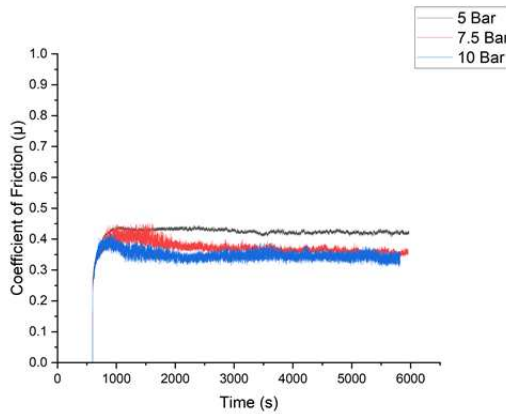


Fig. 7. COF for 5, 7.5 and 10 bar brake pressure for the Corroded test

turer. The coating made from zinc and aluminium mixtures is used to protect the disc against corrosion while in storage [43]. Figure 8b shows that the protective coating was largely removed during the bedding-in process. The transfer layer on the friction ring of the uncorroded disc, shown for increasing pressures in Figure 8c to Figure 8e respectively, becomes darker and more apparent. The development of the tribolayer improves and stabilises the COF [44, 45], as can be seen in Figure 6 for the 7.5 and 10 bar tests when compared to the 5 bar test.

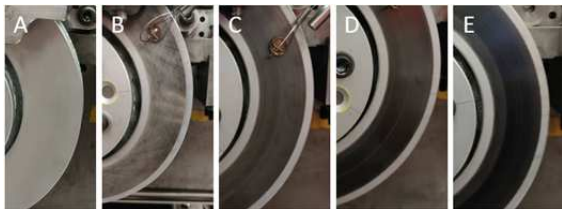


Fig. 8. Timeline of uncorroded brake disc: A) New brake disc, B) After bedding-in, C) After 5 bar, D) After 7.5 bar and E) after 10 bar

Figure 9 presents the surface of the corroded brake disc. Figure 9a and Figure 9b show the brake disc friction ring

and vent after it had been in the salt spray bath for 96 hours. A large build-up of corrosion product can be seen on the friction ring. Corrosion was also found inside the vents of the brake disc despite the protective coating. This may be due to the difference in thermal expansion between the substrate material and the coating which creates cracks in the coating during the brake application [46].

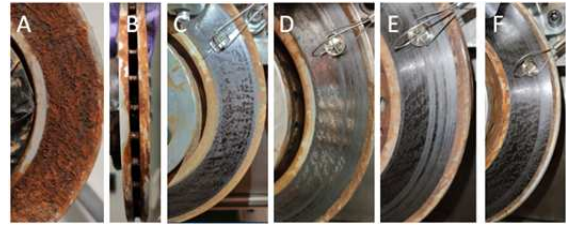


Fig. 9. Timeline of corroded brake disc: A, B) After 96h in the salt spray brake disc, C) After bedding-in, D) After 5 bar, E) After 7.5 bar and F) after 10 bar

Surface topography images of the uncorroded and corroded brake disc taken using vertical-scanning white interferometry (Bruker NpFlex) after the bedding-in procedure are shown in Figure 10. Figure 10a shows the surface topography of the uncorroded disc, from which remaining machining marks from the manufacturing process can be seen. Also, the surface of the disc appears relatively flat, which allows for a large and even contact area between the brake pad and disc. Figure 10b shows small cavities and pits in the corroded disc surface and the uneven surface topography suggests a reduced true area of contact with the brake pad. This could be one of the reasons why the COF presented for the corroded disc in Figure 7 is lower than for the uncorroded disc presented in Figure 6. The Bruker NpFlex also measured the average surface roughness of the uncorroded disc to be $0.587 \mu\text{m}$ whereas for the corroded disc it had increased to $0.719 \mu\text{m}$.

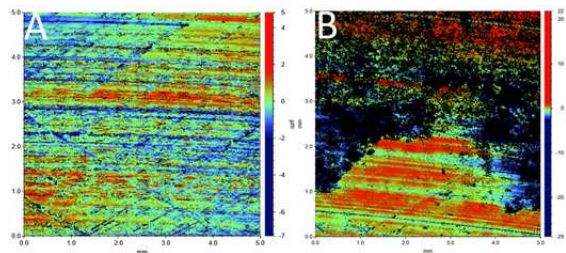


Fig. 10. Surface topography of A) uncorroded disc and B) corroded disc using Bruker NpFlex

5.3 Particle emission

The particle number and mass generated from the uncorroded and corroded discs at each brake pressure as measured by the Dekati ELPI+ are presented in Figure 11 and Figure 12 respectively. For simplicity, the brake wear emissions have been coarsely categorised into particle size ranges of PM10 and PM2.5. Although it is more usual to consider only particle mass at these higher size ranges, the particle number measurements are included in the results

presented below for completeness. For the uncorroded test, Figure 11 (left), the 7.5 bar pressure produced the highest number of wear particles in the PM2.5 category, closely followed by 5 bar whilst 10 bar produced the lowest number of wear particles. For the corroded tests, 7.5 bar produced the most wear particles followed by 5 bar and then 10 bar. Overall, the 7.5 bar corroded test produced the highest number of PM2.5 wear particles and the 10 bar uncorroded test produced the lowest number of PM2.5 wear particles. Figure 11 (right) shows that the uncorroded test of 5 bar produced the highest number of wear particles in the PM10 category followed by 7.5 and then 10 bar which produced the lowest number of PM10 wear particles. This trend is as expected from the COF results since the 5 bar produced the highest COF followed by 7.5 bar and then 10 bar. However, for the corroded test, the 10 bar pressure produced the highest number of PM10 wear particles followed by 7.5 bar and lastly 5 bar with the lowest number of PM10 wear particles. Most importantly, the corroded disc produced significantly more wear particles in both PM2.5 and PM10 categories than the uncorroded disc across all 3 brake pressures tested.

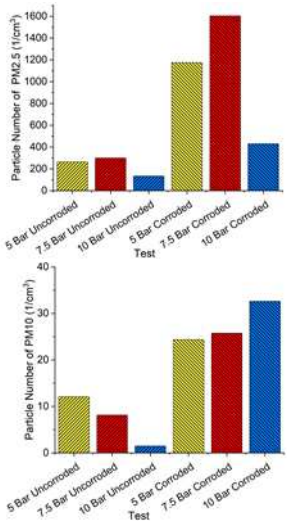


Fig. 11. Number of wear particles in PM2.5 (top) and PM10 (bottom) size

From Figure 12, it can be seen that the 5 bar pressure produced the highest PM2.5 particle mass in the uncorroded test followed by 7.5 bar and then 10 bar with the least amount of wear particle mass. For the corroded rotor, 5 bar produced the highest PM2.5 particle mass, followed by 10 bar and 7.5 bar, respectively. In the case of the PM10 category, 5 bar produces the highest particle mass for the uncorroded test followed by 7.5 bar and then 10 bar where the mass produced was again very small. In contrast, for the corroded disc, 10 bar shows the highest PM10 particle mass followed by the 7.5 bar and the 5 bar pressure which has the least PM10 particle mass. It should be noted that, for the corroded disc, the difference in PM10 particle mass for the three brake pressures was quite small.

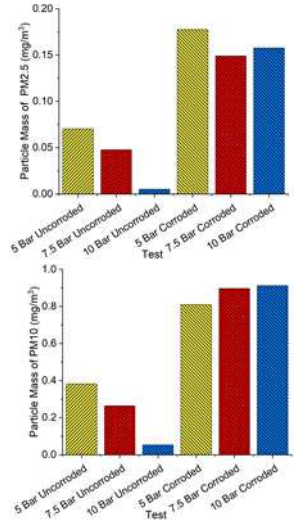


Fig. 12. Mass of wear particles in PM2.5 (top) and PM10 (bottom) size

5.4 Brake Pad wear loss measurements

Figure 13 shows the average dimensional wear measurements of the brake pads at each braking pressure with the brake disc in both the uncorroded and corroded conditions. Of the uncorroded tests, 5 bar produced the highest brake pad wear, which correlates with the high COF for this brake pressure. 10 bar and 7.5 produced lower pad wear loss presumably at least partly due to the lower COF produced for these higher pressures. The fact that 10 bar produced higher pad wear than the 7.5 bar tests despite having lower COF could be due to the higher disc surface temperature measured at 10 bar. In the corroded tests, 7.5 bar produced the highest pad wear, and 10 and 5 bar produced slightly lower pad wear. However, these differences are small and probably not statistically significant, unlike the uncorroded tests where there are clear differences for the different pressures. It could be that the high and consistent pad wear for the corroded tests is driven by the rough and uneven surface of the corroded disc rather than by any differences in measured COF and brake temperature.

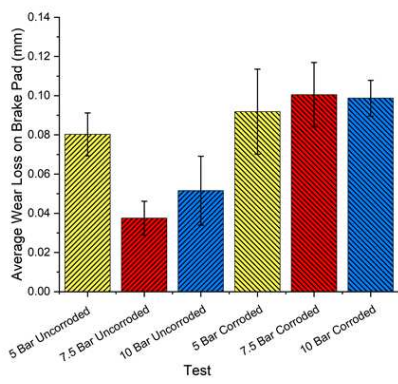


Fig. 13. Brake pad wear loss measurement

6 Discussion

GCI is known to be highly corrosive in most environments, therefore it was not unexpected for it to severely corrode when subjected to 96 hours in a salt spray cabinet. The impact of corrosion on the surface condition, braking performance and particle emissions of the severely corroded GCI brake disc are now compared with those of the uncorroded disc. Figure 14 and Figure 15 show the average steady-state brake temperature and COF, respectively, for both uncorroded and corroded discs at each brake pressure. The error bars are the standard deviation of the individual test results. Figure 14 shows that the steady-state brake temperature for the corroded disc is consistently lower than for its uncorroded counterpart. This is expected due to the fact the steady-state COF for the corroded disc is consistently lower than for the uncorroded disc as shown in Figure 15. Going back to the fundamentals of how friction retards a vehicle by converting kinetic energy into heat through friction, and given that the applied pressure and rotational speed in these drag braking tests are constant, then the heat generated should be directly proportional to the effective COF at the rubbing interface [37].

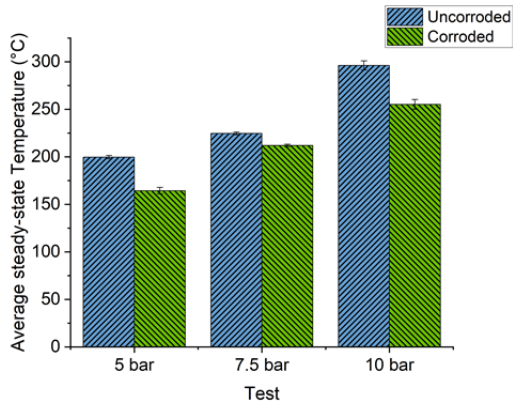


Fig. 14. Steady-state brake temperature of each brake pressure before and after the brake disc was corroded

One potential reason for the deduction in COF for the corroded disc shown in Figure 15 is that the real contact area between the brake pad and disc has been reduced due to the corrosion crevices on the surface of the brake disc, as shown in Figure 10b. In contrast, the uncorroded brake disc was relatively flat and with no obvious crevices or pits on the surface. For the corroded disc, the reduction in real contact area may have reduced the friction force generated at the sliding interface even though the nominal contact area and pressure are the same [47]. Moreover, the corrosion crevices in the surface of the brake disc and the resulting increased surface roughness may have disrupted the formation of the tribolayer on the disc which acts to stabilise friction [48].

Figure 16 shows the percentage increases in the number of particles in the PM10 and PM2.5 categories for the corroded disc compared with the uncorroded baseline values. Despite 5 bar producing the lowest percentage increase in

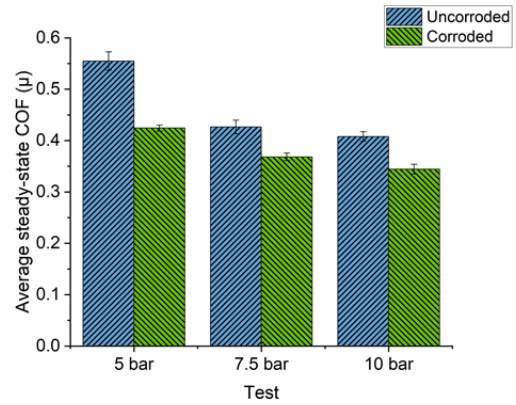


Fig. 15. Steady-state brake COF at each brake pressure before and after the brake disc was corroded

the PM10 category, approximately 50% more wear particles are still emitted compared with the uncorroded disc under the same test conditions. In the case of the 10 bar pressure, the highest percentage increase of about 95% was obtained in the PM10 category despite this pressure giving the lowest COF out of all tests. The increases in the PM2.5 category are more consistent within the range of around 70 to 80% compared with the uncorroded disc test results.

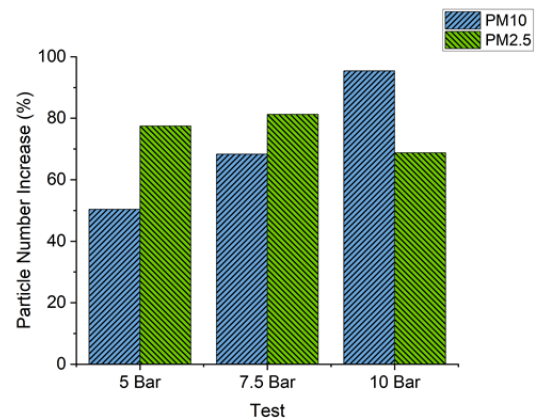


Fig. 16. Percentage increase of particle number for the corroded disc

The percentage increase of wear particles mass for the corroded disc is shown in Figure 17. Overall, the percentage increases at each pressure are very similar in both PM10 and PM2.5 size ranges. Again, the lowest percentage increase is around 50% in the PM10 category at 5 bar pressures. The 10 bar test gave the highest percentage mass increase of around 95% in both PM10 and PM2.5 categories.

It is well known that a rough rubbing surface on the brake rotor can impact the tribological properties of the brake system. A study carried out by Okamura et al [49] investigated the effects of different surface textures on a brake disc and considered the tribological behaviour during running-in. It was found that a smooth disc surface had a higher COF due to the adhesive effect. In contrast,

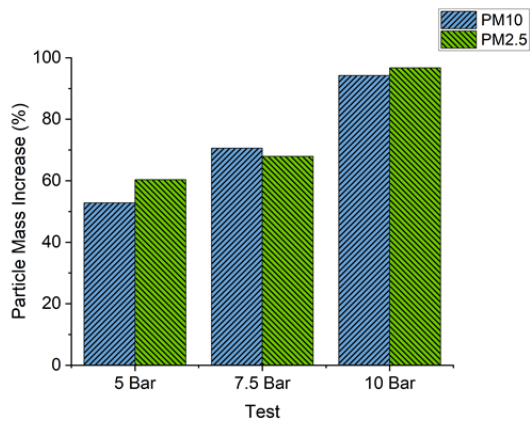


Fig. 17. Percentage increase of particle mass for the corroded disc

a brake disc with a rough surface has smaller areas of real contact with the friction material resulting in lower COF. The present study found that COF decreased as the brake pressure increased for both uncorroded and corroded discs as presented in Figure 15. Djafri et al. [42] investigated the influence of normal load on the coefficient of friction and found that as the normal load increased the coefficient decreased. The reason for this was attributed to the condition of the tribolayer formed between the brake pad and disc. The brake pressure, type of friction material and interface temperature are all known to be factors that affect the tribolayer [50]. Wei et al. [51] also reported a similar reduction in COF with increased pressure and explained that this is possibly due to a non-proportional change of local pressure on asperities due to the properties of the friction materials. Another factor for lower COF at higher pressures could be due to the increase in surface temperature. Rhee et al. [52] also found that as temperature increased, the tribolayer or friction film became softer and less viscous which led to lower COF. The present study shows that, as the brake pressure increases, the particle mass emissions decrease. A similar study carried out by Asmawi et al. [30] found that the particle mass emissions in the PM10 category also decreased as the brake pressure increased. This decreasing particle mass with the increase of brake pressure could be attributed to the reduction in COF at higher brake pressures which was also reported by Asmawi et al. [30]. The influences of the tribolayer not only affects the braking performance but also the formation of surface corrosion. Molina et al [25] found that the formation of corrosion of the surface of the brake disc is not only dependent on the surface material, but also on the tribolayer formed during the bedding-in process. As the brake pad was believed to be a low-metallic friction material, this could explain the formation of cervices on the surface, as low metallic brake pads contain abrasive metal fibres. The present corroded tests produced lower steady-state COF and higher wear loss than the uncorroded test. It was suggested above that this was caused by the reduced contact area between pad and disc. Another factor that could contribute to the low COF and increased wear of the corroded disc is the formation and

breakdown of the tribolayer. Candeo et al. [53] found that the dynamic formation and disruption of the tribolayer will result in increased wear. As the tribolayer tries to develop during braking, the crevices in the corroded surface may prevent this by acting as a channel for the wear particles for example, resulting in an increase in wear particles and a reduction in COF. The disruption of the tribolayer can also be attributed to the increase in wear particles emitted. The uncorroded brake disc performed much better than the corroded disc by producing higher COF but having lower particle emissions. In contrast, the corroded disc produced lower COF but had over a 50% increase in particle number and mass emissions. The increase in wear particles could be linked to the disruption of the tribolayer [48, 54, 55]. The trapped wear particles generated from braking are released into the environment due to cervices and pits providing a release route. Nogueira et al. [56] investigated the friction, wear and particle emission of copper-free friction material and found that the particle emissions rate is linked to the characteristic of the tribolayer. It was found that the growth of the tribolayer is dependent on the availability of wear particles. However, as the tribolayer is disrupted, it allows the wear particle in the friction layer to become airborne.

7 Summary/Conclusions

From the current study, the clear overall trend in terms of braking performance is that after 96 hours of exposure to the salt spray solution, the corroded disc consistently produced significantly lower COF and disc surface temperature than the uncorroded disc. However, the corroded disc tests produced at least a 50% increase in PM2.5 and PM10 emission particle number and mass at 5 bar pressure and up to almost 100% increase in PM10 particle number and mass at the highest pressure of 10 bar. There are at least 2 potential reasons for this very significant increase in particle emission for the corroded disc: (1) the salt spray solution produces corrosion products (mainly iron oxides) on the surface of the GCI disc that are easily removed during brake application to increase the emitted PM, (2) even after most of these loose corrosion products have been removed, the surface of the disc remains rougher and with obvious crevices and pits which inhibit the formation of a stable tribolayer and also increase the PM emissions from the pad as indicated by the pad wear measurements reported above. As electric vehicles increase their dependency on the regenerative braking system, this will lead to a reduction in the average pressures applied to the friction brakes when braking in different scenarios. From the results presented in the paper, more emissions are produced by these lower pressures, especially if the brake disc is corroded. The fact that the friction brakes will be used less frequently and less severely on EV's makes it more likely that the disc surface will become, and will remain longer, in the corroded condition giving rise to significantly higher emissions than would otherwise be the case.

8 Future work

future investigation will consist of:

1. The analysis of chemical composition generated from the collected brake wear particle emissions from both uncorroded and corroded discs
2. Inducing corrosion of brake pads and rotor when held in contact with each other (as when the vehicle is parked)
3. Investigating braking performance and particle emissions of more abrasive brake pad material on the corroded GCI brake rotor
4. Conduct corroded brake tests on different lightweight and coated brake rotor materials
5. Convert the Leeds dynamometer to an inertial test bench so that variable speed braking cycles such as WLTP can be carried out.

9 References

- [1] BBC, “Ban on new petrol and diesel cars in UK from 2030 under PM’s green plan - BBC News.” <https://www.bbc.co.uk/news/science-environment-54981425> (accessed Jun. 30, 2021).
- [2] “Norway to ‘completely ban petrol powered cars by 2025’ The Independent.” www.independent.co.uk/climate-change/news/norway-to-ban-the-sale-of-all-fossil-fuelbased-cars-by-2025-and-replace-with-electric-vehicles-a7065616.html (accessed Feb. 12, 2022).
- [3] “Which countries have banned petrol and diesel cars?” <https://news.trust.org/item/20201118095737-8h1uh> (accessed Feb. 12, 2022).
- [4] “These Are The Countries Moving The Fastest To Ban Combustion Engine Cars.” <https://www.hotcars.com/fastest-countries-to-ban-combustion-engine-cars/> (accessed Feb. 12, 2022).
- [5] “Pollution warning over car tyre and brake dust - BBC News.” <https://www.bbc.co.uk/news/business-48944561> (accessed Dec. 03, 2019).
- [6] OECD, Non-exhaust Particulate Emissions from Road Transport. OECD, 2020.
- [7] BBC, “‘London throat’: Toxic brake dust could cause condition, scientists say BBC News,” <https://www.bbc.co.uk/news/uk-england-london-51049326> (accessed Jan. 25, 2020).
- [8] P. Monks et al., “AIR QUALITY EXPERT GROUP. Non-Exhaust Emissions from Road Traffic,” p. 51014, 2013, [Online]. Available: <http://uk-air.defra.gov.uk>.
- [9] K. T. Chau, “Pure electric vehicles,” in *Alternative Fuels and Advanced Vehicle Technologies for Improved Environmental Performance*, Elsevier, 2014, pp. 655—684.
- [10] M. K. Yoong et al., “Studies of regenerative braking in electric vehicle,” *IEEE Conf. Sustain. Util. Dev. Eng. Technol.* 2010, STUDENT 2010 - Conf. Bookl., no. November, pp. 40—45, 2010, doi: 10.1109/STUDENT.2010.5686984.
- [11] J. Wahlström et al., “A study of the effect of brake pad scorching on tribology and airborne particle emissions,” *Atmosphere (Basel)*, vol. 11, no. 5, 2020, doi: 10.3390/ATMOS11050488.
- [12] “Electric Car Regenerative Braking — Volkswagen UK.” <https://www.volkswagen.co.uk/en/electric-and-hybrid/sustainability/brake-energy-recuperation.html> (accessed Feb. 13, 2022).
- [13] “Regenerative braking — Drive modes — Starting and driving — XC40 Recharge Pure Electric 2021 — Volvo Support.” <https://www.volvocars.com/uk/support/manuals/xc40-recharge-pure-electric/2020w37/starting-and-driving/drive-modes/regenerative-braking> (accessed Feb. 13, 2022).
- [14] K. Liu et al., “Deicing efficiency analysis and economic-environment assessment of a novel induction heating asphalt pavement,” *J. Clean. Prod.*, vol. 273, p. 123123, Nov. 2020, doi: 10.1016/j.jclepro.2020.123123.
- [15] F.-Y. Ma, “Corrosive Effects of Chlorides on Metals,” in *Pitting Corrosion*, InTech, 2012.
- [16] X. Chu, M. Qing, and Y. Wang, “Effect of chloride ion on metal corrosion behavior under pinhole defect of coating studied by wbe technology,” *Corros. Prot.*, vol. 40, no. 1, pp. 23—27, 2019, doi: 10.11973/fsyfh-201901005.
- [17] C. Houska, “Deicing Salt—Recognizing The Corrosion Threat,” *TMR Consult*. Pittsburgh, PA USA, pp. 1—11, 2007.
- [18] K. E. Heusler, D. Landolt, and S. Trasatti, “Electrochemical corrosion nomenclature,” *Pure Appl. Chem.*, vol. 61, no. 1, pp. 19—22, 1989, doi: 10.1351/pac198961010019.
- [19] S. A. Johnston et al., “Brake Testing Methodology Study - Driver Effects Testing,” vol. 47, no. March, p. 51, 1999.
- [20] L. L. SHREIR, “Basic Concepts of Corrosion,” in *Corrosion*, Elsevier, 1976, pp. 1:3-1:15.
- [21] W. Tait Stephen, *An introduction to electrochemical corrosion testing for practicing engineers and scientists*. 1996.

- [22] G. Cueva, A. Sinatora, W. L. Guesser, and A. P. Tschiptschin, "Wear resistance of cast irons used in brake disc rotors," *Wear*, vol. 255, no. 7—12, pp. 1256—1260, Aug. 2003, doi: 10.1016/S0043-1648(03)00146-7.
- [23] S. Venkatesh and K. Murugapoopathiraja, "Scoping Review of Brake Friction Material for Automotive," *Mater. Today Proc.*, vol. 16, pp. 927—933, 2019, doi: 10.1016/j.matpr.2019.05.178.
- [24] K. A. CHANDLER and J. C. HUDSON, "Iron and Steel," in *Corrosion*, Elsevier, 1976, pp. 3:3-3:20.
- [25] N. Molina Montasell and B. Ferrer, "Brake Rotor Corrosion and Friction Cleaning Effect on Vehicle Judder Performance," in *SAE Technical Papers*, Sep. 2019, vol. 2019-Sept, no. September, pp. 1—10, doi: 10.4271/2019-01-2115.
- [26] K. H. Cho et al., "Corrosion induced brake torque variation: The effect from gray iron microstructure and friction materials," *SAE Tech. Pap.*, no. 724, 2005, doi: 10.4271/2005-01-3919.
- [27] M. K. A. Hamid, A. M. Kaulan, S. Syahrullail, and A. R. A. Bakar, "Frictional characteristics under corroded brake discs," *Procedia Eng.*, vol. 68, pp. 668—673, 2013, doi: 10.1016/j.proeng.2013.12.237.
- [28] "'Air pollution' particles linked to Alzheimer's found in human brain." <https://www.telegraph.co.uk/news/2016/09/05/air-pollution-particles-linked-to-alzheimers-found-in-human-brain/> (accessed Jan. 31, 2020).
- [29] M. Gasser et al., "Toxic effects of brake wear particles on epithelial lung cells in vitro," *Part. Fibre Toxicol.*, vol. 6, no. 1, p. 30, Dec. 2009, doi: 10.1186/1743-8977-6-30.
- [30] A. Sanuddin, C. Gilkeson, P. Brooks, S. Kosarieh, D. Barton, and S. Shrestha, "Preliminary Comparisons of Particulate Emissions Generated from Different Disc Brake Rotors," 2021, pp. 1—7, [Online]. Available: <https://eprints.whiterose.ac.uk/177272/>.
- [31] S. Gramstat, R. Waninger, D. Lugovyy, and M. Schröder, "Friction couple investigations in terms of brake particle emissions," *Eurobrak 2018*, pp. 1—15, 2018.
- [32] A. Mancini et al., "Chemistry of the Brake Emissions: Influence of the Test Cycle," Oct. 2021, pp. 1—9, doi: 10.4271/2021-01-1300.
- [33] D. Hesse, C. Hamatschek, K. Augsburg, T. Weigelt, A. Prahst, and S. Gramstat, "Testing of Alternative Disc Brakes and Friction Materials Regarding Brake Wear Particle Emissions and Temperature Behavior," *Atmosphere (Basel)*, vol. 12, no. 4, p. 436, Mar. 2021, doi: 10.3390/atmos12040436.
- [34] T. Budinsky, P. Brooks, and D. Barton, "A new prototype system for automated suppression of disc brake squeal," *Proc. Inst. Mech. Eng. Part D J. Automob. Eng.*, vol. 235, no. 5, pp. 1423—1433, Apr. 2021, doi: 10.1177/0954407020964624.
- [35] Dekati, "Dekati ® ELPI + User Manual," 2016.
- [36] S. P. ASTM, "B 0117 Operating Salt Spray (Fog) Apparatus," *Astm*, pp. 1—12, 2011, doi: 10.1520/B0117-11.2.
- [37] A. Day, *Braking of Road Vehicles*. 2014.
- [38] SAE International, "Brake Pads, Lining, Disc, and Drum Wear Measurements (SAE J2986)," *SAE Int.*, 2019, doi: https://doi.org/10.4271/J2986_01901.
- [39] W. Y. Loh, R. H. Basch, D. Li, and P. Sanders, "Dynamic modeling of brake friction coefficients," *SAE Tech. Pap.*, vol. 110, pp. 2627—2636, 2000, doi: 10.4271/2000-01-2753.
- [40] A. W. Orłowicz, M. Mróz, G. Wnuk, O. Markowska, W. Homik, and B. Kolbusz, "Coefficient of Friction of a Brake Disc-Brake Pad Friction Couple," *Arch. Foundry Eng.*, vol. 16, no. 4, pp. 196—200, Dec. 2016, doi: 10.1515/afe-2016-0109.
- [41] D. Hesse and C. Hamatschek, "Investigations on the Deposition Behaviour of Brake Wear Particles on the Wheel Surface," pp. 1—13, 2021, doi: 10.4271/2021-01-1301.Abstract.
- [42] M. Djafri, M. Bouchetara, C. Busch, and S. Weber, "Effects of humidity and corrosion on the tribological behaviour of the brake disc materials," *Wear*, vol. 321, pp. 8—15, Dec. 2014, doi: 10.1016/j.wear.2014.09.006.
- [43] Ferodo, "COAT+ Brake Discs — Ferodo." <https://www.ferodo.co.uk/products/light-vehicles/brake-discs/coat-brake-discs.html> (accessed May 26, 2022).
- [44] S. K. Rhee, M. G. Jacko, and P. H. S. Tsang, "The role of friction film in friction, wear and noise of automotive brakes," *Wear*, vol. 146, no. 1, pp. 89—97, May 1991, doi: 10.1016/0043-1648(91)90226-K.
- [45] J. O. Chung, S. R. Go, J. H. Kim, H. R. Kim, and H. B. Choi, "Conditions for Transfer Film Formation and Its Effect on Friction Coefficients in NAO Friction Materials Containing Various Abrasive Components," *Int. J. Precis. Eng. Manuf.*, vol. 19, no. 7, pp. 1011—1017, 2018, doi: 10.1007/s12541-018-0119-7.
- [46] O. Aranke, W. Algenaid, S. Awe, and S. Joshi, "Coatings for Automotive Gray Cast Iron Brake Discs: A Review," *Coatings*, vol. 9, no. 9, p. 552, Aug. 2019, doi: 10.3390/coatings9090552.

[47] R. L. Machado Pinto, J. C. Horta Gutiérrez, R. B. D. Pereira, P. E. de Faria, and J. C. C. Rubio, "Influence of Contact Plateaus Characteristics Formed on the Surface of Brake Friction Materials in Braking Performance through Experimental Tests," *Materials (Basel)*, vol. 14, no. 17, p. 4931, Aug. 2021, doi: 10.3390/ma14174931.

[48] H. Rajaei, M. Griso, C. Menapace, A. Dorigato, G. Perricone, and S. Gialanella, "Results in Materials Investigation on the recyclability potential of vehicular brake pads," *Results Mater.*, vol. 8, no. November, p. 100161, 2020, doi: 10.1016/j.rinma.2020.100161.

[49] T. Okamura and M. Ono, "Effect of Brake Disc Surface Texture on Friction Behavior during Running-in," in *SAE Technical Papers*, Oct. 2004, no. 724, doi: 10.4271/2004-01-2765.

[50] F. Gulden, A. Stich, S. Gramstat, H. W. Höppel, and M. Göken, "Fundamental Investigations of Aluminium Matrix Brake Rotors for the Use in Passenger Cars," 2017.

[51] L. Wei, Y. S. Choy, and C. S. Cheung, "A study of brake contact pairs under different friction conditions with respect to characteristics of brake pad surfaces," *Tribol. Int.*, vol. 138, no. April, pp. 99—110, Oct. 2019, doi:10.1016/j.triboint.2019.05.016.

[52] S. Rhee, D. Sharma, S. R. Singh, and A. Rathee, "An Investigation of the Role of Wear and Friction Film Influencing the Friction Coefficient of Brakes: Mechanism of Brake Fade," in *SAE Technical Paper Series*, Oct. 2020, vol. 1, pp. 1—17, doi: 10.4271/2020-01-1630.

[53] S. Candeo, A. P. Nogueira, M. Leonardi, and G. Straffelini, "A study of friction, wear and particulate emissions during the bedding stage of a Cu-free friction material," *Wear*, vol. 486—487, no. September, p. 204095, Dec. 2021, doi: 10.1016/j.wear.2021.204095.

[54] A. Sinha, G. Ischia, C. Menapace, and S. Gialanella, "Experimental Characterization Protocols for Wear Products from Disc Brake Materials," *Atmosphere (Basel)*, vol. 11, no. 10, p. 1102, Oct. 2020, doi: 10.3390/atmos11101102.

[55] L. Y. Barros et al., "Effect of pressure in the transition between moderate and severe wear regimes in brake friction materials," *Wear*, vol. 438—439, no. August, p. 203112, Nov. 2019, doi: 10.1016/j.wear.2019.203112.

[56] A. P. G. Nogueira, M. Leonardi, G. Straffelini, and S. Gialanella, "Sliding Behavior and Particle Emissions of Cu-Free Friction Materials with Different Contents of Phenolic Resin," *Tribol. Trans.*, vol. 63, no. 4, pp. 770—779, Jul. 2020, doi: 10.1080/10402004.2020.1753870.

10 Contact Information

Ishmaeel Ghouri, University of Leeds Email: mn18ihg@leeds.ac.uk

11 Acknowledgements

I would like to thank all my supervisors David Barton, Richard Barker, Shahriar Kosarieh and Peter Brooks for all their guidance. I would also like to thank Tony Wiese and the technicians at the University of Leeds for their support.